Geophysical Research Letters

RESEARCH LETTER
10.1029/2022GL101826

Key Points:

- The perturbed parameter ensemble mean captures the climate pattern of the Asian summer monsoon (ASM) but mainly overestimates precipitation over the western Pacific
- Four parameters (*ent_fac_dp*, *qlmin*, *ps_cloud-ph*, and *psm*) are crucial for simulating ASM precipitation in coupled run
- The joint effect of these parameters, especially the deep entrainment amplitude, are dominant control for the bias in the western Pacific

Supporting Information:

Supporting Information may be found in the online version of this article.

Correspondence to:

B. He,
heb@lasg.iap.ac.cn

Citation:

Zhang, X., He, B., Guo, Z., Sexton, D. M. H., Rostron, J. W., & Furtado, K. (2023). Sensitivities of the Asian summer monsoon simulations to physical parameters for the perturbed parameter ensemble of HadGEM3-GC3.05. *Geophysical Research Letters*, *50*, e2022GL101826. https://doi.org/10.1029/2022GL101826

Received 20 OCT 2022
Accepted 6 MAY 2023

Sensitivities of the Asian Summer Monsoon Simulations to Physical Parameters for the Perturbed Parameter Ensemble of HadGEM3-GC3.05

Xiaoqi Zhang[1,2], Bian He[1,3], Zhun Guo[1,4], David M. H. Sexton[5], John W. Rostron[5], and Kalli Furtado[5]

[1]State Key Laboratory of Numerical Modeling for Atmospheric Sciences and Geophysical Fluid Dynamics (LASG), Institute of Atmospheric Physics (IAP), Chinese Academy of Sciences, Beijing, China, [2]Nanjing University of Information Science and Technology, Nanjing, China, [3]University of Chinese Academy of Sciences, Beijing, China, [4]Climate Change Research Center, Chinese Academy of Sciences, Beijing, China, [5]Met Office Hadley Centre, Exeter, UK

Abstract The simulation skill of the perturbed parameter ensemble (PPE) of HadGEM3-GC3.05 on the mean climate pattern of the Asian summer monsoon (ASM) is evaluated in this study. The sensitivities of the model bias to the perturbed parameters are investigated based on metrics. The results show that the PPE mean (PPE-20M) could effectively capture the general ASM precipitation and wind patterns, with a correlation coefficient of 0.78. PPE-20M mainly shows positive precipitation biases over the tropical western Pacific, southern slope of the Tibetan Plateau, Indochina Peninsula, and South China and negative precipitation biases over the Indian continent and Bay of Bengal. The magnitude of the precipitation biases is more sensitive than its pattern to the variation of the perturbed parameters. Four parameters (*ent_fac_dp*, *qlmin*, *ps_cloud-ph*, and *psm*) are found to be crucial for simulating the ASM precipitation intensity, and their combined effects are related to the simulated precipitation biases.

Plain Language Summary The simulation of the Asian summer monsoon (ASM) has attracted much attention in recent decades. However, state-of-the-art coupled models still show similar systematic biases when simulating monsoon precipitation from CMIP3 to CMIP6. Recently, a perturbed parameter ensemble (PPE) method has been applied in the development of HadGEM3-GC3.05 with the aim of improving the overall simulation skill of the coupled model. The PPE can also be used to understand the related physical processes in the model simulations. Thus, in this study, we aim to evaluate the simulation skills of PPE on the mean climate distributions of ASM. Four parameters were found to be the most critical in the precipitation simulations, which could be potential tunable parameters to reduce the biases of precipitation intensity over the monsoon regions. This study provides possible pathways to reduce model bias that could benefit the model development community.

1. Introduction

In the most significant monsoon region on Earth, the precipitation variabilities associated with the Asian summer monsoon (ASM) affect the daily lives of nearly 60% of the global population. The simulations and predictions of Asian monsoon precipitation attract much interest but encounter tremendous challenges. For example, the interannual variabilities observed in the Asian monsoon precipitation over land have been poorly represented in a series of projects since the late 20th century, such as the Atmospheric Model Intercomparison Project (Gates, 1992; Gates et al., 1999) and the Climate Variability and Predictability (CLIVAR) International Climate of the 20th Century Project (C20C) (Folland et al., 2002, 2014; Kinter & Folland, 2011; Li et al., 2007). In the above projects, atmospheric models were forced by observed sea surface temperature (SST) and sea ice concentration data. Air-sea interactions were not considered, though these factors are important for simulating land-sea thermal contrasts in Asian monsoon regions in these kinds of experiments.

Although some studies have proposed that resolving air-sea interactions could improve the simulation of the Asian monsoon region (Bollasina & Nigam, 2009; Fu et al., 2002; Wang, 2006), state-of-the-art coupled models still show quite large biases when simulating ASM. Sperber et al. (2013) found that the CMIP5 multimodel mean (MMM) is more accurate than the CMIP3 MMM across all diagnostics in terms of its ability to simulate pattern correlations with respect to observations. However, there are still biases in the CMIP5 model simulations,

including rainfall underestimations in the Yangtze River basin and weak western Pacific subtropical high pressures (Feng et al., 2014; Song & Zhou, 2014). Recently, Xin et al. (2020) indicated that CMIP6 models exhibit improved skill scores with regard to the climatological pattern of the East Asian summer monsoon (EASM) relative to the previous CMIP5 models; these improvements are related to the relatively small SST biases of the CMIP6 models over the Northwestern Pacific Ocean. However, the CMIP6 models do have biases in that they report insufficient rainfall in the Yangtze River basin and northwestern Xinjiang Province and excessive rainfall in Northern China, Northwest China and on the Tibetan Plateau (TP).

The uncertainties of physical parameterizations are one of the main sources of model biases. To reduce this kind of model bias and to improve the performance of HadGEM3-GC3.05, the Met Office Hadley Centre recently proposed perturbed parameter ensemble (PPE) simulations (Sexton et al., 2021). By testing nearly 3,000 samples of parameter space in atmosphere-only simulations, 25 variants with combinations of 47 parameters were finally selected to run the global coupled simulations for the 1900–2100 period. Additional five parameters were necessary to be perturbed for maintaining consistency with 5 of the 47 independent parameters, and all 52 of which are listed in Table 1 of Sexton et al. (2021). The preliminary evaluations show that a 20-member PPE (PPE-20) appears to have a good performance when simulating many aspects compared to the CMIP5 models. Moreover, the ensemble shows a large spread of climate variabilities in simulating many aspects of the global climate, such as the El Niño-Southern Oscillation (ENSO) and Atlantic Multi-decadal Oscillation (AMO) (Yamazaki et al., 2021). In general, the selected PPE-20 shows reasonable performance in climate simulations such as climatological averages and internal variability, etc. (Yamazaki et al., 2021). Meanwhile, it provides a useful data set for understanding the different combinations of physical parameters related to physical processes such as convection, aerosol-cloud-radiation interactions, boundary layer heat and moisture transport.

In this paper, we investigate the simulation skill of PPE-20 in reproducing the mean ASM climate pattern from 1979 to 2014. The simulation skill is quantitatively estimated by objective algorithms. Furthermore, the sensitivities of the ASM simulation skill to 52 physical parameters are analyzed. The possible cause and related parameters together with the associated physical processes are further discussed. Additionally, the importance of the parameters in the 518 Atmospheric Model Intercomparison Project (AMIP) samples are shown in the Supporting Information S1 for reference. This study aims to address two main questions: (a) How well does PPE-20 simulate the mean ASM climate precipitation pattern? (b) What are the key parameters and the associated physical processes that relate to the model biases? These analyses will provide a reference for improving model simulations of ASM and will also advance our understanding of ASM dynamics. The following study is divided into three sections. Section 2 introduces the data sets and methods. Section 3 presents the results of the evaluation. Section 4 presents the conclusions and discussion.

2. Data Sets and Methods

2.1. Observation Data Sets

The Global Precipitation Climatology Project (GPCP) Version 2 (V2) data set, a monthly global precipitation data set containing data recorded from January 1979 to December 2014, is used for this study (Adler et al., 2003; Huffman et al., 2009). It is a 2.5° × 2.5° gridded data set that combines satellite estimates and rain gauge data.

The ERA5 wind reanalysis data produced by the European Center for Medium-Range Weather Forecasting (ECMWF) from January 1979 to December 2014 are also used in this study (Hersbach et al., 2020).

2.2. PPE Data Sets

In this study, the 20-member PPE of the UK Hadley Centre Unified Model HadGEM3-GC3.05 model was used for global coupled simulations, which is conducted for the 1900–2100 period forced by CMIP5 historical and RCP8.5 emissions (Sexton et al., 2021; Yamazaki et al., 2021). Each ensemble member has a horizontal resolution of approximately 60 km at mid-latitudes and was run for a 200-year period from 1900 to 2100. The 52 parameters perturbed for the PPE simulations are related to physical processes, such as convection, gravity wave drag, boundary layers, cloud radiation, cloud microphysics, aerosols, and land surface and snow (Table 1 in Sexton et al., 2021). Before being used, all data were interpolated to 2.5° × 2.5° resolution, and the period from 1979 to 2014 was selected for evaluation in this study.

Before running the coupled model, the same parameters are perturbed in the AMIP type run firstly (Sexton et al., 2021). This is a viable method of using relatively inexpensive atmospheric experiments to identify model parameter combination variants that can be applied in coupled model runs. The atmospheric experiment uses time-varying CO_2 concentrations from CMIP5 and prescribed SST and sea ice from the HadISST2 observational data set (Titchner & Rayner, 2014) for the period December 2004 to November 2009. The atmospheric experiment has 518 ensemble members. They have the same resolution as the ensemble members of the coupled model. Before being used, all data were interpolated to 2.5° × 2.5° resolution. The analysis of the AMIP simulations is presented in Supporting Information S1.

2.3. Methods

The simulation skills are calculated by the following metrics:

(1) The standard deviation (σ_x)

The term σ_x is the standard deviation of the simulated variable (x) and is calculated as follows:

$$\sigma_x = \sqrt{\frac{1}{N}\sum_{i=1}^{N}\left(x_i - \overline{x}\right)^2} \tag{1}$$

where i is one of different horizontal grid points (or precipitation in different ensemble members), N is the number of horizontal grid points (or the number of ensemble members), and $\overline{x}$ is the mean of variable x (Guo et al., 2014; Yang et al., 2013).

(2) Correlation coefficient (R)

R is the correlation coefficient between two variables and is calculated as follows:

$$R = \frac{\frac{1}{N}\sum_{i=1}^{N}\left(x_i - \overline{x}\right)\left(y_i - \overline{y}\right)}{\sqrt{\frac{1}{N}\sum_{i=1}^{N}\left(x_i - \overline{x}\right)^2}\sqrt{\frac{1}{N}\sum_{i=1}^{N}\left(y_i - \overline{y}\right)^2}} \tag{2}$$

where x_i is the precipitation at different grid points (or the values of the parameter from different ensemble members), y_i is the reference variable at one of many grid points (or simulation skills), and $\overline{y}$ is the mean of variable y (Guo et al., 2014; Yang et al., 2013).

(3) Root mean square error of correlation and standard deviation ratio (RMSE-CSD)

To quantify the bias of the simulation, we use RMSE-CSD to measure the model bias between the model simulations and observations, as has been adopted in past studies (Zhang et al., 2022). The formula is described as follows:

$$\mathrm{RMSE-CSD} = \sqrt{(1-R)^2 + \left(1 - \frac{\sigma_x}{\sigma_y}\right)^2} \tag{3}$$

where R is the spatial correlation coefficient between the models and observed data and σ_x/σ_y is the standard deviation ratio between the model field and the observed field. Spatial correlation coefficients and standard deviation ratios are two important parameters for evaluating model simulations using Taylor plots (Taylor, 2001).

(4) Generalized linear model (GLM)

A GLM was used herein to analyze the responses of the perturbed parameters, including their linear and nonlinear interaction effects. The GLM assumes that the response of precipitation is a linear function of those multiple perturbed parameters:

$$Y = \beta_0 + \sum_{j=1}^{n}\beta_j * p_j + \sum_{j=1}^{n}\sum_{k=1}^{n}\beta_{j,k} * p_j * p_k + \varepsilon, \varepsilon \sim N\left(0, \sigma^2\right) \tag{4}$$

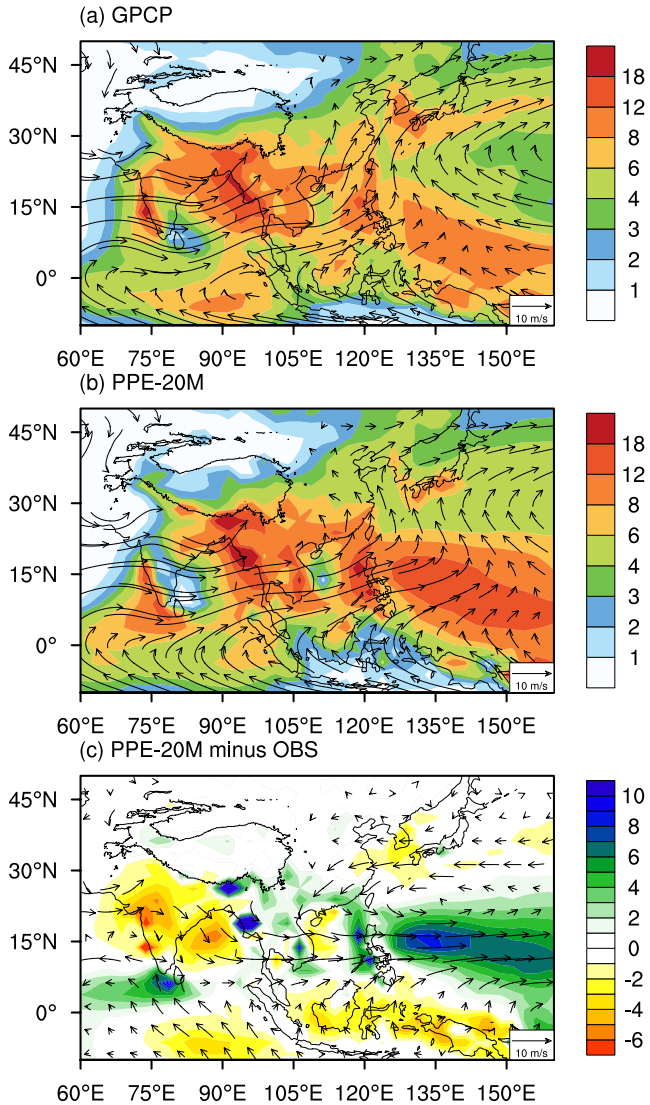

Figure 1. Precipitation (shaded; unit: mm day^{-1}) and 850-hPa wind (vector; unit: m s^{-1}) climatology for boreal summer (JJA) from 1979 to 2014 in the Global Precipitation Climatology Project/ERA5 (a) and PPE-20M (b) results. Model biases in 850-hPa winds and precipitation are also shown (c).

where Y represents the response variable (e.g., precipitation); p_j represents the jth parameter; β_j and $\beta_{j,k}$ represent the coefficients of linear and two-way interaction terms, respectively; and ε denotes the residual and follows an independent normal distribution with a zero mean and unit variance (Guo et al., 2014; Qian et al., 2015).

The GLM establishes the fitting equations by estimating the maximum likelihood between the parameter (p) and the simulation (Y). The GLM calculates the coefficient of determination (R^2) of the model fitness, interpreted variance, and the P-value for each parameter. C_j, C_{ind}, C_{int} are used to represent the relative contribution of the jth parameter, the sum of the contributions of all selected parameters and the sum of the relative contributions of the interacting terms between each pair of the parameters, respectively. The reduction in residual sum square caused by each parameter (or all selected parameters or two interacting parameters) is used to calculate its relative contribution (C_j, C_{ind}, C_{int}) (Guo et al., 2014; Qian et al., 2015).

3. Results

3.1. PPE-20 Ensemble Mean Simulations

We first investigate the PPE-20 ensemble mean (PPE-20M) on the simulations of the climate mean ASM precipitation and 850-hPa wind patterns, as shown in Figure 1. The observed ASM precipitation mainly shows three strong centers (above 12 mm day^{-1}) over the East Arabian Sea, over the Bay of Bengal (BOB) and south slope of the TP, and over the South China Sea and Philippine Islands. The monsoon rainbelt (above 4 mm day^{-1}) extends north to mid-high latitudes over the East Eurasian continent. The monsoon airflow shows a strong westerly over the subtropical Indian Ocean regions and turns northward over East Asia. Over the western Pacific, there is an obvious anticyclone that indicates the location of the Western Pacific High (WPH). Strong precipitation over the western Pacific is mainly located within the latitude band of 0–15°N, south of the WPH. The simulation bias obtained herein is similar to the results of HadGEM3's AMIP experiment (Wong et al., 2018), and the reason for this bias may not be related to sea-air interactions.

The PPE-20M reproduced the large-scale ASM precipitation and low-level wind patterns well (Figure 1b), but overestimated the strength of precipitation over the south slope of the TP and the western Pacific. The model biases are shown in Figure 1c. It is clear that the largest positive precipitation bias occurs over the tropical western Pacific. Moreover, the model overestimated precipitation over the southern slope of the TP and Indo-China Peninsula (ICP) and mainly underestimated precipitation over the Indian subcontinent and BOB in the ASM region. The 850-hPa wind biases mainly appear as anomalously strong westerlies from the Indian Ocean to the western Pacific Ocean, with a cyclonic anomaly over East Asia and the midlatitude western Pacific. We infer that the airflow bias may transport excessive water vapor from the Indian Ocean to the western Pacific and may contribute to the precipitation bias.

3.2. Simulation Skills of the PPE-20 Members

We analyze the ensemble spread and simulation skills of all the members in this subsection. It is worth noting that the area (10°S–50°N, 60°E–160°E) for calculating the RMSE-CSD and the Taylor diagram are shown in Figure 1. The model biases of PPE-20M are also compared with the biases of the individual ensemble member to further understand their possible causes. First, the quantitative understanding of the ensembles' skill in capturing the ASM precipitation pattern is analyzed with a Taylor diagram in Figure 2. For all ensemble members, the correlation coefficients are larger than 0.6 (Figure 2), indicating that all selected members can basically reproduce the

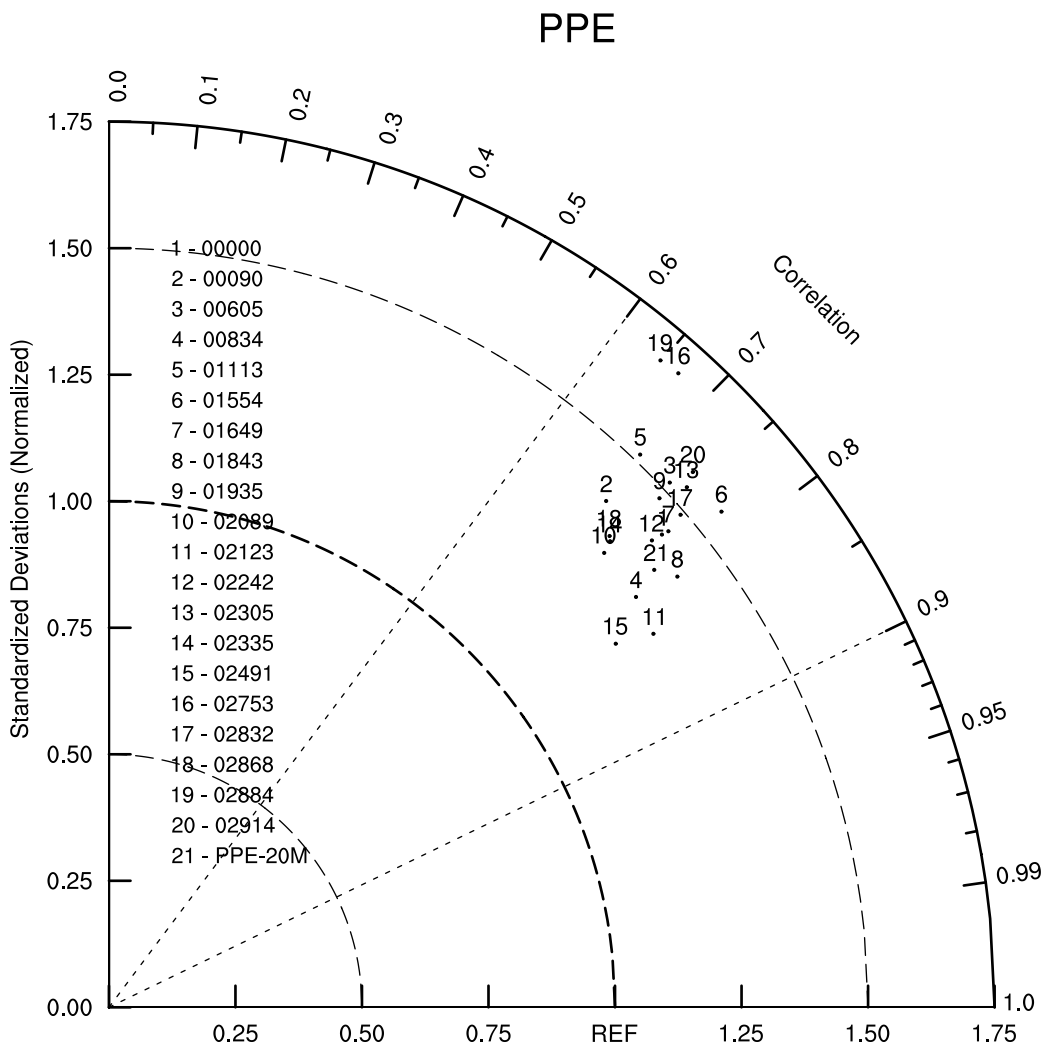

Figure 2. Taylor diagram of all ensemble members and ensemble mean (PPE-20M) for the simulation of boreal summer precipitation in Asia (The region is shown in Figure 1).

large-scale ASM pattern. Moreover, all of the standard deviation ratios are greater than 1 (Figure 2), implying that the intensities of ASM precipitation are overestimated in general for all the ensemble members. Moreover, it is worth noting that the skill of PPE-20M (No. 21 in Figure 2) is not the highest, implying that the ensemble mean is not the best choice for reducing model biases in PPE simulations. It is clear that No. 11 (02123) and No. 15 (02491) show better skills than all the other ensemble members, while No. 19 (02884) shows the lowest skill. Thus, by comparing the model results among these simulations, the sensitivities of the ASM simulation to the perturbed parameters in PPE-20 can be identified.

We use RMSE-CSD (Equation 3) as the metric to comprehensively measure the simulation skill for both the pattern correlation and standard ratio. When the RMSE-CSD is close to 0 (i.e., when the correlation coefficient and standard deviation ratio are close to 1), the ensemble member shows high skill in ASM simulation. The ensemble member (02491) with the highest simulation skill and the ensemble member (02884) with the lowest skill were obtained by ranking the simulation skills in the ASM region (Table S1 in Supporting Information S1). In the following text, we compare the simulations between the members with the highest and lowest skills, as shown in Figure 3. The precipitation patterns obtained using the highest-skill ensemble member (No. 02491) and the lowest-skill ensemble member (No. 02884) are similar overall, except over the Indian subcontinent (Figures 3a and 3c). Compared to the PPE-20M in Figure 1b, No. 02491 captures the intensity of the precipitation over the south slope of the TP and BOB well, while No. 02884 simulates even stronger precipitation biases in these two

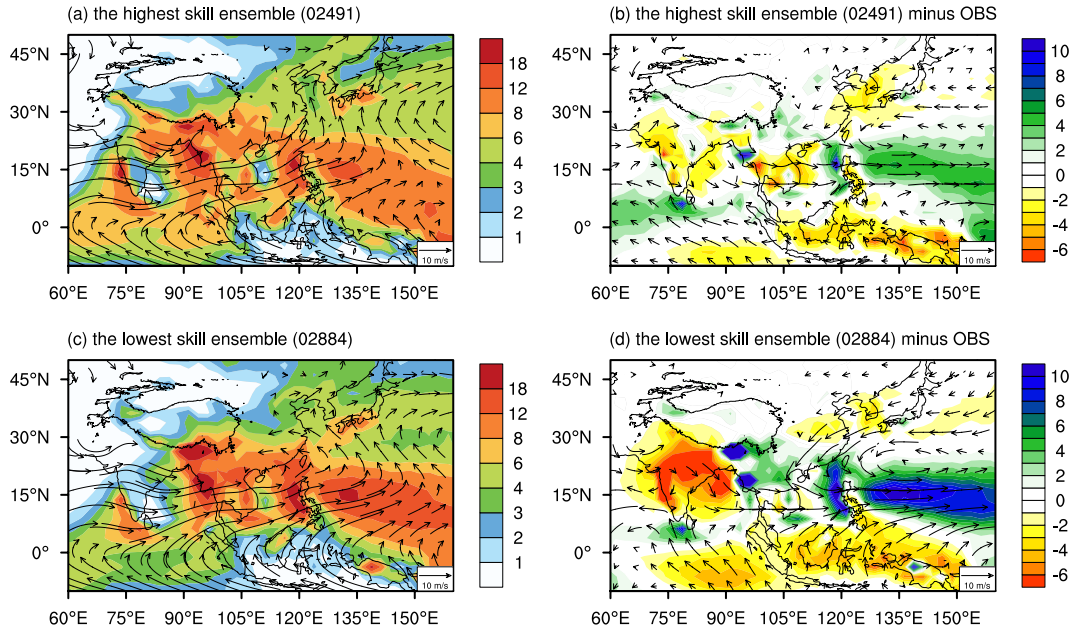

Figure 3. Simulations of precipitation patterns (shaded; unit: mm day^{-1}) and 850-hPa wind fields (vector; unit: m s^{-1}) based on the highest skill ensemble member (No. 02491) (a) and the lowest skill ensemble member (No. 02884) (c) and the corresponding biases (b, d).

places (Figure 3c) than PPE-20M (Figure 1b). Moreover, No. 02884 underestimated precipitation over the Indian subcontinent while overestimating precipitation over the western Pacific.

The biases of the two ensemble members are quantitively calculated in Figures 3b and 3d. In No. 02884 (Figure 3d), the model shows a strong positive precipitation bias in the tropical western Pacific and on the southern slopes of the TP (biases larger than 5 mm day^{-1}), while it shows a strong negative precipitation bias in the Indian subcontinent (biases lower than −5 mm day^{-1}). For the highest skill member (No. 02491), the pattern (Figure 3b) of the precipitation bias was overall similar to that identified with No. 02884 (Figure 3d), but the magnitude was much smaller. In particular, the biases over Eurasian lands are very small, while the positive biases over the tropical western Pacific are overall less than 5 mm day^{-1}. Regarding low-level circulation, both members of PPE simulate a strong westerly wind biases along 15°N, similar to that seen for PPE-20M (Figure 1c). Moreover, No. 02884 shows a strong cyclonic circulation bias over the tropical western Pacific (Figure 3d), indicating that the WPH is very weak and the high pressure center is also off in this case. We further investigated the SST biases in these cases (Figure S2 in Supporting Information S1). The results show that the strong positive precipitation bias in the tropical western Pacific is accompanied by a cold SST bias in the ensemble (Figure S2d in Supporting Information S1). Precipitation in southern China had a positive correlation with the Indian Ocean surface temperature and a negative correlation with the tropical western Pacific surface temperature, consistent with the results of Chang et al. (2013). Previous observations also revealed that the correlations between precipitation and SST are negative in the western Pacific (Lu & Lu, 2014). The increase in precipitation in the tropical western Pacific is not triggered by a locally warm SST (Chang et al., 2013; Lu & Lu, 2014). This negative correlation is the result of SST response to the atmospheric influences (Lu & Lu, 2014). Uncertainties in the atmospheric model physics should be the main cause of this kind of bias. In the next section, we analyze the 52 perturbed parameters in PPE-20 and determine the connections between these perturbed parameters and the precipitation biases.

3.3. Sensitivity of the ASM Precipitation Simulation to the Perturbed Parameters

To understand the influence of a single perturbed parameter on the ASM precipitation simulations, we calculated the linear correlations (Equation 2) between the RMSE-CSD and the values in the 20 ensemble runs for each of the 52 parameters, and the correlations of four parameters passed the 90% significance level of the Student's T-test (Figure 4), indicating that the ASM precipitation simulation and associated model biases are significantly sensitive to these four parameters. Among the four parameters, the RMSE-CSD was positively correlated with

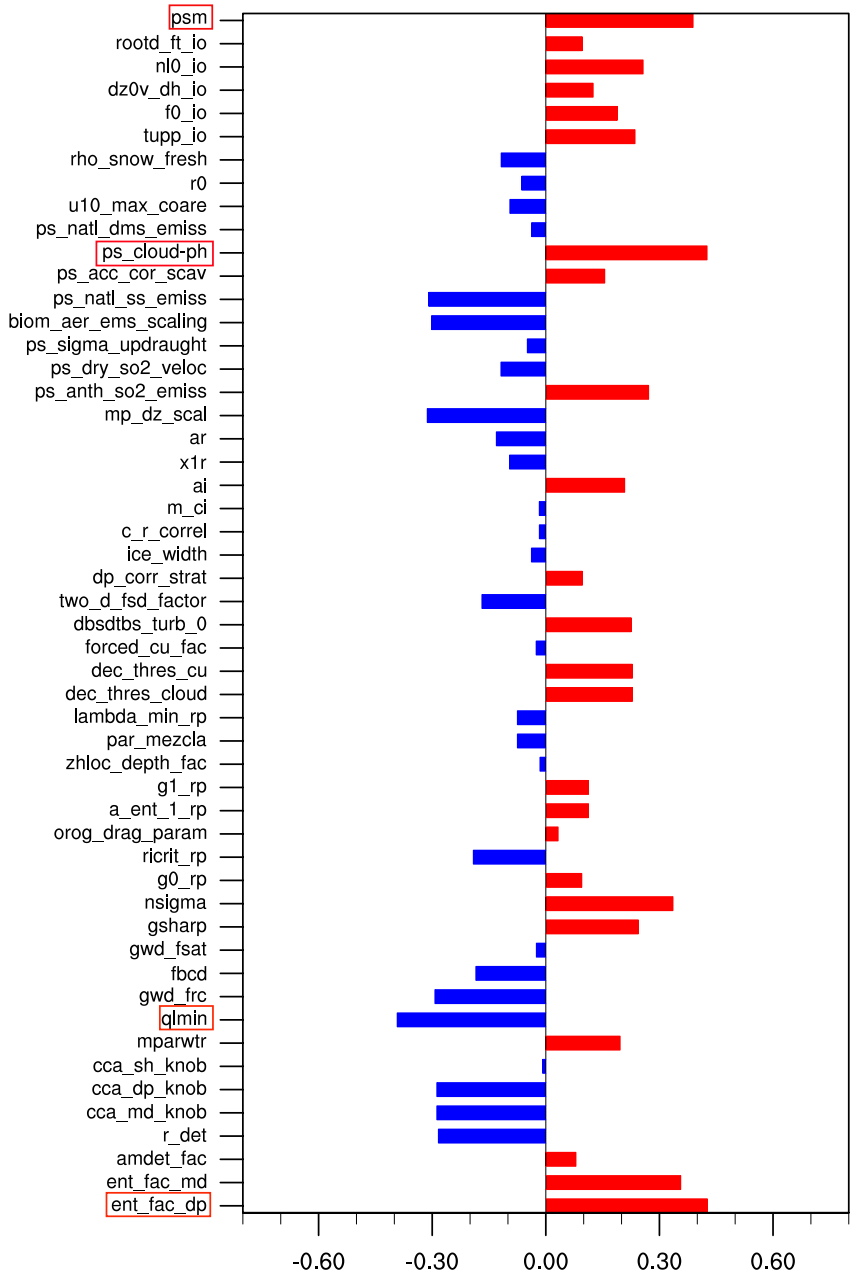

Figure 4. Linear correlations between the model simulation Root mean square error of correlation and standard deviation ratio and 52 parameters. Variables with red boxes indicate that the correlations of these parameters passed the 90% significance level of the Student's T-test.

three parameters (*ent_fac_dp*, *ps_cloud-ph* and *psm*), while one parameter (*qlmin*) was negatively correlated with RMSE-CSD. The parameter "*ent_fac_dp*," "*qlmin*," *"ps_cloud-ph*," and *"psm"* denote "the deep entrainment amplitude," "the minimum critical cloud condensate, which is the minimum value of the function that defines the maximum amount of condensation a convective parcel can hold before it is converted into precipitation," "the pH of cloud drops and is used to control in-cloud SO_4^{2-} production dependent on SO_2 availability," and "scaling factor for critical and saturation soil moisture levels toward the wilt level" (Table S2 in Supporting Information S1; Table 1 in Sexton et al., 2021). Increasing the value of the "*ent_fac_dp*" will reduce the depth of convection and suppress active precipitating convection. Reducing the value of the "*qlmin*" will cool the troposphere, while increasing it will warm the troposphere by altering the amount of high clouds. Increasing the value of the "*ps_cloud-ph*" will lead to faster SO_2 oxidation by ozone in cloud water, so more SO_4^{2-} production will occur. The

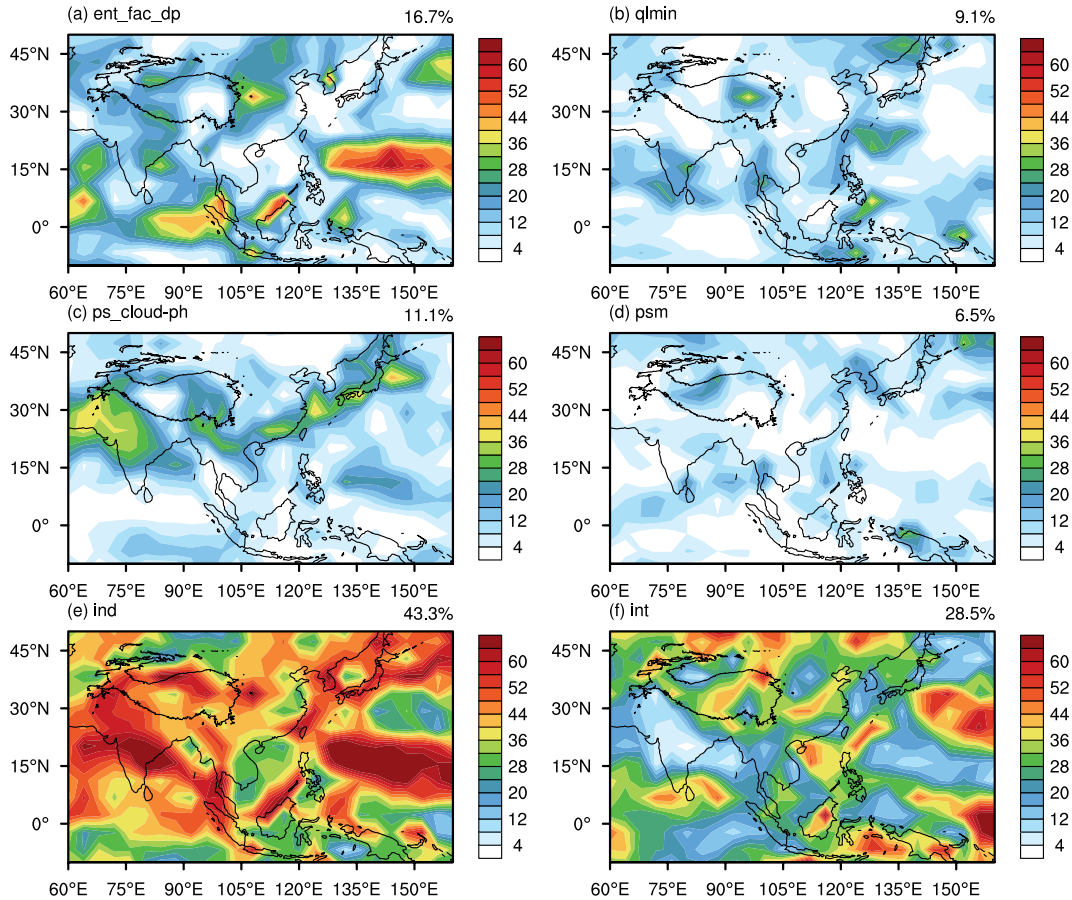

Figure 5. Relative contributions of the four analyzed parameters to precipitation in Asia (C_j) (shaded; unit: %) (a–d). The sum of the relative contributions of the four parameters to Asian precipitation (C_{ind}) (shade; unit: %) (e). The sum of the contributions of the interacting terms between each pair of the parameters to precipitation in Asia (C_{int}) (shaded; unit: %) (f). The number in the upper right corner indicates the regional average.

higher value of the "*psm*" will lead to larger soil moisture regimes where soil moisture limits evapotranspiration, with consequent implications for moisture and surface energy fluxes (Sexton et al., 2021).

Box plots are provided in Figure S3 in Supporting Information S1 for understanding the distributions of the above four parameters. The parameter values obtained in the highest-skill case (No. 02491) and lowest-skill case (No. 02884) are marked with blue and red dots, respectively. It is clear that the highest-skill simulation was associated with lower *ent_fac_dp*, *ps_cloud-ph*, and *psm* values and a higher *qlmin* value. This result indicates that the reduced convection depth and suppressed precipitation, increased threshold of the condensation of convective parcels (more clouds and water vapor and less condensation), decreased pH in cloud drops to reduce the SO_4^{2-} contents, and evapotranspiration could improve the simulations of moist convection, cloud-aerosol radiation, and processes. This will contribute to the overall skill of the ASM simulation and reduce the biases of the precipitation simulation in HadGEM3 GC3.05. To further understand the joint contributions of these four parameters to the simulation of the Asian summer precipitation pattern, the GLM method was applied (Equation 4) to quantitively calculate the single and joint contributions of the parameters to the precipitation simulations in Figure 5. It is clear that *ent_fac_dp* is closely connected with the precipitation simulation (contributions amounted to 16.7%). In particular, this parameter contributes more than 50% in the western Pacific, where the positive precipitation biases are large (Figure 5a). Similar conclusions can be drawn from the large ensemble of AMIP experiments, thus demonstrating the robustness of the contribution of this parameter to precipitation biases (Figures S5–S8 in Supporting Information S1). The *ps_cloud-ph* parameter mainly shows an influence over the western Indian subcontinent, south TP, south China and northwest Pacific, with a total contribution of 11.1% (Figure 5c). This parameter may contribute to precipitation biases over the low-latitude Asian continent and adjacent ocean

regions. Moreover, it seems that this parameter is closely connected with the dry bias over India in No. 02884. When this parameter is large, more SO_4^{2-} is produced, associated with less clouds and less precipitation (Figure S4 in Supporting Information S1). The contributions of the other two parameters (Figures 5b and 5d) alone are relatively small. The influences of the joint contributions of the total four parameters (Figure 5e) are the largest and of the joint contributions of any two combinations of these four parameters (Figure 5f) are larger than the individual one. These three (qlmin, ps_cloud-ph, psm) contributions to precipitation biases may only become more significant in air-sea coupled runs, since their contributions in AMIP runs are very limited (Figure S7 in Supporting Information S1). It is obvious that the joint contributions of these four parameters can contribute up to 43.3% of the summer precipitation biases. Thus, these four parameters are the key tunable parameters in HadGEM3-GC3.05 when simulating the intensity of ASM precipitation.

4. Conclusions and Discussions

In this study, the ASM simulation skill of the PPE-20 was investigated for use in HadGEM3-GC3.05. The PPE-20 mean could basically reproduce the large-scale pattern of ASM precipitation but mainly overestimated precipitation over the western Pacific, underestimated precipitation over the Indian subcontinent and simulated an overall strong monsoonal westerly along 15°N. Further analysis suggested that the precipitation biases are sensitive to four parameters (*ent_fac_dp*, *qlmin*, *ps_cloud-ph*, and *psm*) in the model. A decrease in *ent_fac_dp* could effectively reduce precipitation biases over the tropical western Pacific, while a decrease in *ps_cloud-ph* could favor the occurrence of precipitation over the Indian subcontinent in fully coupled runs. The joint contributions of these four parameters contribute 43.3% of the summer precipitation biases, and these parameters can be used as the key tuning parameters to improve the overall performance of ASM simulations in future studies. However, we need to mention that in this study, precipitation was the variable targeted with the goal of understanding the sensitivity to the physical model parameters. Notably, that the westerly wind biases identified along 15°N are not very sensitive to the analyzed parameters, and the possible causes for this need further study.

Data Availability Statement

The ERA5 data set utilized herein is available at https://cds.climate.copernicus.eu/cdsapp#!/dataset/reanalysis-era5-pressure-levels-monthly-means?tab=overview. The GPCP precipitation data set utilized herein is available at http://www.esrl.noaa.gov/psd/data/gridded/data.gpcp.html. The PPE-20 data are available by arrangement with the Met Office, please use the enquiry form at https://www.metoffice.gov.uk/forms/contact-us-ukcp18.

Acknowledgments
We would like to thank the two anonymous reviewers for their constructive suggestions, which helped to improve the overall quality of the manuscript. The research presented in this paper is jointly funded by the National Key Research and Development Program of China (Grant 2020YFA0608903), the National Natural Science Foundation of China (Grants. 42122035, 42288101, and 91937302), the UK- China Research & Innovation Partnership Fund through the Met Office Climate Science for Service Partnership (CSSP) China, and the Guangdong Major Project of Basic and Applied Basic Research (Grant 2020B0301030004). The calculation of this study was supported by the National Key Scientific and Technological Infrastructure project "Earth System Numerical Simulation Facility" (EarthLab).

References

Adler, R. F., Huffman, G. J., Chang, A., Ferraro, R., Xie, P. P., Janowiak, J., et al. (2003). The version-2 Global Precipitation Climatology Project (GPCP) monthly precipitation analysis (1979–present). *Journal of Hydrometeorology*, *4*(6), 1147–1167. https://doi.org/10.1175/1525-7541(2003)004<1147:tvgpcp>2.0.co;2

Bollasina, M., & Nigam, S. (2009). Indian Ocean SST, evaporation, and precipitation during the South Asian summer monsoon in IPCC-AR4 coupled simulations. *Climate Dynamics*, *33*(7–8), 1017–1032. https://doi.org/10.1007/s00382-008-0477-4

Chang, E. C., Yeh, S. W., Hong, S. Y., & Wu, R. (2013). Sensitivity of summer precipitation to tropical sea surface temperatures over East Asia in the GRIMs GMP. *Geophysical Research Letters*, *40*(9), 1824–1831. https://doi.org/10.1002/grl.50389

Feng, J., Wei, T., Dong, W., Wu, Q., & Wang, Y. (2014). CMIP5/AMIP GCM simulations of East Asian summer monsoon. *Advances in Atmospheric Sciences*, *31*(4), 836–850. https://doi.org/10.1007/s00376-013-3131-y

Folland, C., Shukla, J., Kinter, J., & Rodwell, M. (2002). The climate of the twentieth century project. *CLIVAR Exchanges*, *7*, 37–39.

Folland, C., Stone, D., Frederiksen, C., Karoly, D., & Kinter, J. (2014). The international CLIVAR Climate of the 20th Century Plus (C20C+) Project: Report of the sixth workshop. *CLIVAR Exchange*, *19*, 57–59.

Fu, X., Wang, B., & Li, T. (2002). Impacts of air–sea coupling on the simulation of mean Asian summer monsoon in the ECHAM4 model. *Monthly Weather Review*, *130*(12), 2889–2904. https://doi.org/10.1175/1520-0493(2002)130<2889:ioasco>2.0.co;2

Gates, W. L. (1992). AN AMS continuing series: Global CHANGE–AMIP: The atmospheric model intercomparison project. *Bulletin of the American Meteorological Society*, *73*(12), 1962–1970. https://doi.org/10.1175/1520-0477(1992)073<1962:atamip>2.0.co;2

Gates, W. L., Boyle, J. S., Covey, C., Dease, C. G., Doutriaux, C. M., Drach, R. S., et al. (1999). An overview of the results of the Atmospheric Model Intercomparison Project (AMIP I). *Bulletin of the American Meteorological Society*, *80*(1), 29–56. https://doi.org/10.1175/1520-0477(1999)080<0029:aootro>2.0.co;2

Guo, Z., Wang, M., Qian, Y., Larson, V. E., Ghan, S., Ovchinnikov, M., et al. (2014). A sensitivity analysis of cloud properties to CLUBB parameters in the single-column Community Atmosphere Model (SCAM5). *Journal of Advances in Modeling Earth Systems*, *6*(3), 829–858. https://doi.org/10.1002/2014ms000315

Hersbach, H., Bell, B., Berrisford, P., Hirahara, S., Horányi, A., Muñoz-Sabater, J., et al. (2020). The ERA5 global reanalysis. *Quarterly Journal of the Royal Meteorological Society*, *146*(730), 1999–2049. https://doi.org/10.1002/qj.3803

Huffman, G. J., Adler, R. F., Bolvin, D. T., & Gu, G. (2009). Improving the global precipitation record: GPCP Version 2.1. *Geophysical Research Letters*, *36*(17), L17808. https://doi.org/10.1029/2009gl040000

Kinter, J., & Folland, C. (2011). The international CLIVAR Climate of the 20th Century project: Report of the Fifth Workshop. *CLIVAR Exchanges*, *57*, 39–42.

Li, L., Wang, B., & Zhou, T. (2007). Impacts of external forcing on the 20th century global warming. *Chinese Science Bulletin*, *52*(22), 3148–3154. https://doi.org/10.1007/s11434-007-0463-y

Lu, R., & Lu, S. (2014). Local and remote factors affecting the SST–precipitation relationship over the western North Pacific during summer. *Journal of Climate*, *27*(13), 5132–5147. https://doi.org/10.1175/jcli-d-13-00510.1

Qian, Y., Yan, H., Hou, Z., Johannesson, G., Klein, S., Lucas, D., et al. (2015). Parametric sensitivity analysis of precipitation at global and local scales in the Community Atmosphere Model CAM5. *Journal of Advances in Modeling Earth Systems*, *7*(2), 382–411. https://doi.org/10.1002/2014ms000354

Sexton, D. M., McSweeney, C. F., Rostron, J. W., Yamazaki, K., Booth, B. B. B., Murphy, J. M., et al. (2021). A perturbed parameter ensemble of HadGEM3-GC3.05 coupled model projections: Part 1: Selecting the parameter combinations. *Climate Dynamics*, *56*(11–12), 3395–3436. https://doi.org/10.1007/s00382-021-05709-9

Song, F., & Zhou, T. (2014). The climatology and interannual variability of East Asian summer monsoon in CMIP5 coupled models: Does air–sea coupling improve the simulations? *Journal of Climate*, *27*(23), 8761–8777. https://doi.org/10.1175/jcli-d-14-00396.1

Sperber, K. R., Annamalai, H., Kang, I. S., Kitoh, A., Moise, A., Turner, A., et al. (2013). The Asian summer monsoon: An intercomparison of CMIP5 vs. CMIP3 simulations of the late 20th century. *Climate Dynamics*, *41*(9–10), 2711–2744. https://doi.org/10.1007/s00382-012-1607-6

Taylor, K. E. (2001). Summarizing multiple aspects of model performance in a single diagram. *Journal of Geophysical Research*, *106*(D7), 7183–7192. https://doi.org/10.1029/2000jd900719

Titchner, H. A., & Rayner, N. A. (2014). The Met Office Hadley Centre sea ice and sea surface temperature data set, version 2: 1. Sea ice concentrations. *Journal of Geophysical Research: Atmospheres*, *119*(6), 2864–2889. https://doi.org/10.1002/2013jd020316

Wang, B. (2006). *The Asian monsoon* (787 pp.). Springer.

Wong, K. C., Liu, S., Turner, A. G., & Schiemann, R. K. (2018). Different Asian monsoon rainfall responses to idealized orography sensitivity experiments in the HadGEM3-GA6 and FGOALS-FAMIL global climate models. *Advances in Atmospheric Sciences*, *35*(8), 1049–1062. https://doi.org/10.1007/s00376-018-7269-5

Xin, X., Wu, T., Zhang, J., Yao, J., & Fang, Y. (2020). Comparison of CMIP6 and CMIP5 simulations of precipitation in China and the East Asian summer monsoon. *International Journal of Climatology*, *40*(15), 6423–6440. https://doi.org/10.1002/joc.6590

Yamazaki, K., Sexton, D. M., Rostron, J. W., McSweeney, C. F., Murphy, J. M., & Harris, G. R. (2021). A perturbed parameter ensemble of HadGEM3-GC3.05 coupled model projections: Part 2: Global performance and future changes. *Climate Dynamics*, *56*(11–12), 3437–3471. https://doi.org/10.1007/s00382-020-05608-5

Yang, B., Qian, Y., Lin, G., Leung, L. R., Rasch, P. J., Zhang, G. J., et al. (2013). Uncertainty quantification and parameter tuning in the CAM5 Zhang-McFarlane convection scheme and impact of improved convection on the global circulation and climate. *Journal of Geophysical Research: Atmospheres*, *118*(2), 395–415. https://doi.org/10.1029/2012jd018213

Zhang, X., He, B., Liu, Y., Bao, Q., Zheng, F., Li, J., et al. (2022). Evaluation of the seasonality and spatial aspects of the Southern Annular Mode in CMIP6 models. *International Journal of Climatology*, *42*(7), 3820–3837. https://doi.org/10.1002/joc.7447